JACS
JOURNAL OF THE AMERICAN CHEMICAL SOCIETY
pubs.acs.org/JACS
Communication

Strong Circularly Polarized Luminescence at 1550 nm from Enantiopure Molecular Erbium Complexes

Nishya F. M. Mukthar, Nathan D. Schley, and Gaël Ung*

Cite This: J. Am. Chem. Soc. 2022, 144, 6148−6153
Read Online

ACCESS | Metrics & More | Article Recommendations | Supporting Information

ABSTRACT: Circularly polarized luminescence (CPL) in two subregions of the near-infrared (NIR) has been achieved. By leveraging the rigidity and diminishing detrimental vibrations of the heterobimetallic binolate complexes of erbium [$(Binol)_3ErNa_3$], species exhibiting an exceptionally high dissymmetry factor ($|g_{lum}|$) of 0.47 at 1550 nm were obtained. These erbium complexes are the first reported examples of CPL observed beyond 1200 nm. Analogous complexes of ytterbium and neodymium also exhibited strong CPL ($|g_{lum}|$ = 0.17, 0.05, respectively) in a higher energy NIR window (800−1200 nm). All complexes exhibit high quantum yields (Er: 0.58%, Yb: 17%, Nd: 9.3%) and high B_{CPL} values (Er: 57 M^{-1} cm^{-1}, Yb: 379 M^{-1} cm^{-1}, Nd: 29 M^{-1} cm^{-1}). Because of their strong CPL emission in the telecom band (1550 nm), biologically relevant NIR emission window (800−1100 nm), and synthetic versatility, the complexes reported here could permit further promising developments in quantum communication technologies and biologically relevant sensors.

Downloaded via UNIV OF CONNECTICUT on August 26, 2022 at 15:34:12 (UTC).
See https://pubs.acs.org/sharingguidelines for options on how to legitimately share published articles.

The 1550 nm wavelength is critical for long-distance telecommunication, as the so-called "1550 nm telecom band" presents very low transmission loss in optical fibers.[1] When combined with polarization control, promising applications in quantum network[2] and quantum communication technologies[3] can be expected. Circularly polarized luminescence (CPL) is the preferential emission of light with right- or left-handed circular polarization. Generating CPL in the telecom band would therefore be highly desirable. Synthesis of molecules emitting CPL has grown in interest[4] due to their potential in improving spintronic devices,[5] enhancing security inks,[6] and generating three-dimensional displays.[7] CPL is quantified by the luminescence dissymmetry factor ($-2 \leq g_{lum} \leq +2$, where $g_{lum} = +2$ indicates pure left-handed CPL). Obtaining high dissymmetry factors in molecular complexes remains challenging, as one of the primary conditions (i.e., similar magnitude in magnetic dipole transition and electric dipole transition moments) is often hard to achieve. Lanthanide-based complexes have been the most successful at generating high dissymmetry factors, particularly for luminescent transitions that are electric dipole forbidden, and magnetic dipole allowed (e.g., Eu $^5D_0 \rightarrow {}^7F_1$).[8] Erbium possesses a luminescent transition ($^4I_{13/2} \rightarrow {}^4I_{15/2}$) that fulfills the latter criterion,[9] and more importantly emits around 1550 nm, making it an excellent candidate for the aforementioned applications.

Luminescence from near-infrared emitting lanthanides such as erbium is challenging, since (1) weak absorbances must be overcome, and (2) quenching for vibrational C−H overtones must be avoided. The weak absorbances can be overcome by the so-called antenna effect, where an appropriate chromophore can be ligated to the lanthanide. We recently modified the so-called Shibasaki complexes [$(Binol)_3LnM_3$] into the reduced [$(H_8{-}Binol)_3LnM_3$] to match the energy levels of lanthanide emitting in the visible region.[10] Since the emissive level of erbium is much lower than the visible lanthanide emitters, we reasoned that the original nonreduced binolate complexes could be well-suited for erbium emission. In addition, we hypothesized that the loss of any C_{sp3}−H vibrations and overall rigidity of the system could prevent some quenching. Recently, other air-stable binolate-lanthanide complexes with nonalkali metal cations (notably tetramethylguanidinium) have been reported;[11] however, to minimize additional quenching, we decided to prioritize the use of an alkali-metal and targeted [$(Binol)_3ErNa_3$].

In addition, due to the potential applications of NIR luminescence in medical imaging,[12] and owing to our interests in luminescence in other regions of the near-infrared (NIR),[13] we also targeted other lanthanide-NIR-emitters: ytterbium and neodymium. We describe herein the synthesis and chiroptical properties of NIR-emitting lanthanide complexes [$(Binol)_3LnNa_3$] (Ln = Er, Yb, and Nd). Both erbium and ytterbium complexes show very strong chiroptical properties ($|g_{lum}|$ = 0.47, 0.17, respectively). The erbium complexes represent the first reported examples of CPL observed beyond 1200 nm.

We synthesized the [$(Binol)_3LnNa_3$] (Ln = Er, Yb, and Nd) utilizing modified literature procedures (Figure 1, see Supporting Information), and isolated the three pairs of enantiomers. While the complexes of ytterbium and neodymium were previously characterized,[11e,14] this is the first report of the erbium analogue. We thus perform single crystal

Received: January 28, 2022
Published: April 4, 2022

© 2022 American Chemical Society

https://doi.org/10.1021/jacs.2c01134
J. Am. Chem. Soc. 2022, 144, 6148−6153

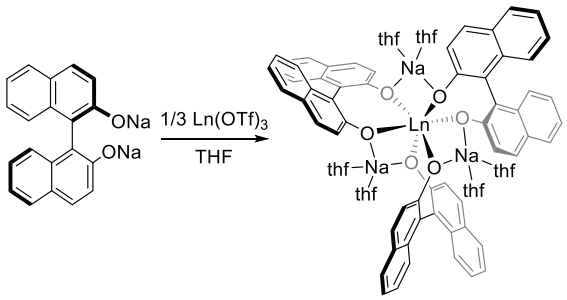

Figure 1. Synthesis of $[(R\text{-Binol})_3LnNa_3(thf)_6]$ (Ln = Er, Yb, Nd) from sodium *R*-Binolate. The corresponding enantiomers are obtained analogously from sodium *S*-Binolate.

X-ray diffraction studies to confirm their identity. As expected, the structures are isomorphous to those previously reported, crystallizing in the noncentrosymmetric $P6_3$ space group. The erbium center is six-coordinate in a distorted trigonal antiprism with the binolate ligands bridged with sodium ions solvated by two molecules of tetrahydrofuran (Figure 2). For the $[(S\text{-Binol})_3ErNa_3(thf)_6]$, the binolate ligands generate a propeller shape at erbium with the Λ-chirality. As expected, the $[(R\text{-Binol})_3ErNa_3(thf)_6]$ shows a propeller shape at erbium with the Δ-chirality.

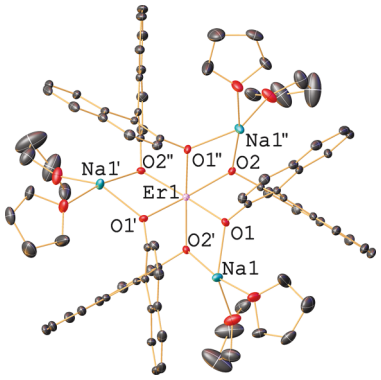

Figure 2. Structure of $[(S\text{-Binol})_3ErNa_3(thf)_6]$ in the solid state. See Figure S20 for the structure of $[(R\text{-Binol})_3ErNa_3(thf)_6]$. Thermal ellipsoids are drawn at 50% probability. Hydrogen atoms are omitted for clarity.

Upon excitation at 380 nm, all complexes exhibited strong NIR luminescence (Figure 3). The erbium complex $[(Binol)_3ErNa_3]$ showed emission ranging from 1430 to 1670 nm arising from the $^4I_{13/2} \rightarrow {}^4I_{15/2}$ transition, with an emission maximum at 1540 nm. We note that due to crystal field splitting, a minimum of four Stark levels are observed. The luminescence of $[(Binol)_3YbNa_3]$ ranged from 930 to 1100 nm with a maximum at 975 nm resulting from the $^2F_{5/2} \rightarrow {}^2F_{7/2}$ transition. The emission spectrum of the neodymium complex $[(Binol)_3NdNa_3]$ showed the expected peaks at 915, 1075, and 1335 nm, from the $^4F_{3/2} \rightarrow {}^4I_{9/2}$, $^4I_{11/2}$, and $^4I_{13/2}$ transitions, respectively. The quantum yields were 0.58%, 17%, and 9.3% for Er, Yb, and Nd, respectively, which are on the high end of other comparable molecular complexes for erbium and neodymium (Er: $\Phi \sim 0.01-2\%$;[15] Yb: $\Phi \sim 4-23\%$[13,16]), and among the highest reported to date for neodymium ($\Phi \sim 0.2-3.2\%$).[15d−f,17]

Circularly polarized luminescence spectra of $[(R/S\text{-Binol})_3ErNa_3]$ were collected in tetrahydrofuran solutions (Figure 4). A tetrasignate pattern was observed with an exceptionally high maximum dissymmetry factor of +0.47 at 1540 nm for $[(S\text{-Binol})_3ErNa_3]$. The spectrum of the enantiomer $[(R\text{-Binol})_3ErNa_3]$ is a perfect mirror image with a dissymmetry factor of −0.47 at 1540 nm. This is the first reported example of CPL observed beyond 1200 nm, and the dissymmetry factors we obtained are among the highest observed for any lanthanides. This result also confirms the prediction made by Zinna and Di Bari, who observed strong circular dichroism from a similar complex.[18] Owing to the strong dissymmetry factors, the calculated CPL brightness of our erbium complexes (B_{CPL} = 57 M^{-1} cm^{-1}) is high, although no comparison can be made with other emitters in this region. The strong chiroptical activities are likely due to a combination of an adequate luminescent transition ($^4I_{13/2} \rightarrow {}^4I_{15/2}$) fitting the high rotatory strength and dissymmetry factor predictions,[9] as well as the presence of both chirality at metal and at ligands. Interestingly, the Stark level centered at 1470 nm does not exhibit strong CPL; this indicates that this transition is unlikely to arise from

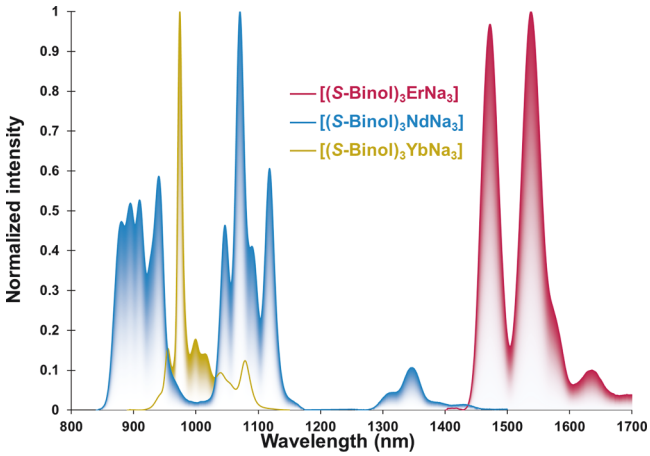

Figure 3. Normalized emission spectra of $[(S\text{-Binol})_3ErNa_3]$ (red), $[(S\text{-Binol})_3YbNa_3]$ (yellow), and $[(S\text{-Binol})_3NdNa_3]$ (blue) in tetrahydrofuran solutions (1.3×10^{-5} mol L^{-1}) at room temperature. Excitation at 380 nm. Bandpass: 26 nm for Er, 4.8 nm for Yb, and 10 nm for Nd.

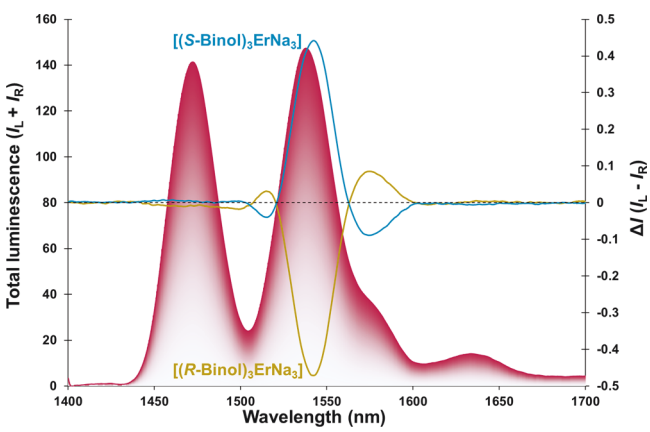

Figure 4. Normalized CPL spectra of $[(R\text{-Binol})_3ErNa_3]$ (yellow) and $[(S\text{-Binol})_3ErNa_3]$ (blue) in tetrahydrofuran solutions (1.3×10^{-3} mol L^{-1}) at room temperature. See Figure S14 for g_{lum} plot. Total luminescence is traced in the background. Excitation at 380 nm. Bandpass: 26 nm.

https://doi.org/10.1021/jacs.2c01134
J. Am. Chem. Soc. 2022, 144, 6148−6153

the zero-line transition, but is rather coming from a higher n' level.

Owing to the strong luminescence of the $[(Binol)_3YbNa_3]$ complexes, CPL spectra were collected with narrow bandpass, increasing resolution of the Stark levels (Figure 5). The $^2F_{5/2}$ and $^2F_{7/2}$ levels of ytterbium can be split by crystal field into three (0′, 1′, 2′) and four (0, 1, 2, 3) doubly degenerate levels, respectively. On the basis of the typical magnitude of the crystal field splitting observed in ytterbium complexes ($\Delta E \sim 300\ cm^{-1}$),[19g,20] all twelve of the transitions from the thermally accessible 0′, 1′, and 2′ states should be observed. Indeed, modeling of the emission profile provided an estimation of the difference in energy between levels, and the population distribution for the excited states (see Figure S30). The spectrum of the $[(S\text{-Binol})_3YbNa_3]$ complex showed a strong dissymmetry factor of +0.17 at 975 nm. Interestingly, a larger dissymmetry factor was observed at 1040 nm ($g_{lum} = -0.19$). These results are on the high end of most Yb-based CPL-emitters reported to date ($0.02 \le g_{lum} \le 0.18$),[15e,f,19] but are marginally lower than the recently reported $CsYb(hfbc)_4$ value ($g_{lum} = 0.38$).[18] We also note that this value is significantly stronger than the one observed by Zinna and Di Bari for an analogous complex $[(S\text{-Binol})_3Yb(TMGH)_3]$ (TMGH = tetramethylguanidinium) ($g_{lum} = 0.066$).[18] Structural comparison between the two species (Na vs TMGH) showed a significant change in the coordination geometry in the solid-state (see Figure S21 and SI for detailed comparison). The behavior in solution is likely to be slightly different, but the large difference in CPL suggests that the sodium cation remains coordinated to the binolates in solution. This highlights the importance of the nature of the cation, a phenomenon reminiscent of what is observed in circular dichroism.[21] The CPL brightness calculated for our complexes ($B_{CPL} = 379\ M^{-1}\ cm^{-1}$) is two orders of magnitude higher than the average B_{CPL} reported for Yb complexes.[22]

While the predicted chiroptical activities of the luminescent transition of neodymium are not expected to be strong,[9] we examined the circularly polarized luminescence of the $^4F_{3/2} \rightarrow {}^4I_{9/2}$ and $^4F_{3/2} \rightarrow {}^4I_{11/2}$ transitions. As expected, the CPL spectrum of $[(S\text{-Binol})_3NdNa_3]$ showed modest chiroptical activity for both transitions ($g_{lum} \le 0.05$, $B_{CPL} \le 29\ M^{-1}\ cm^{-1}$) (Figure 6). Interestingly, in the $^4F_{3/2} \rightarrow {}^4I_{9/2}$, all Stark levels appear to have the same CPL sign, while in the $^4F_{3/2} \rightarrow {}^4I_{11/2}$ transition, a bisignate pattern was observed. This contrasts with the only other reported neodymium CPL spectrum showing bisignate signals for both observed transitions.[19e]

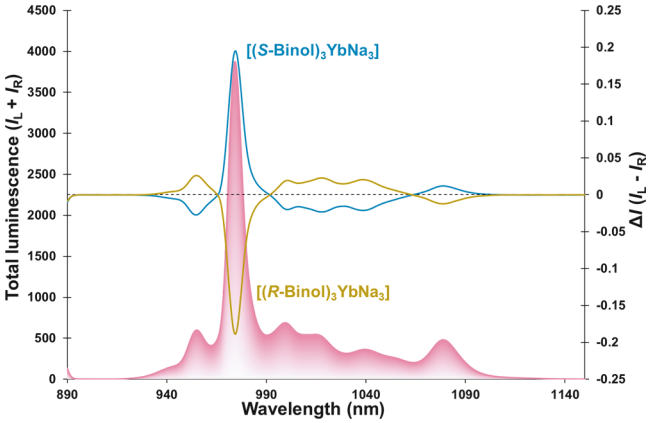

Figure 5. Normalized CPL spectra of $[(R\text{-Binol})_3YbNa_3]$ (yellow) and $[(S\text{-Binol})_3YbNa_3]$ (blue) in tetrahydrofuran solutions (1.3×10^{-3} mol L^{-1}) at room temperature. See Figure S15 for g_{lum} plot. Total luminescence is traced in the background. Excitation at 380 nm. Bandpass: 4.8 nm.

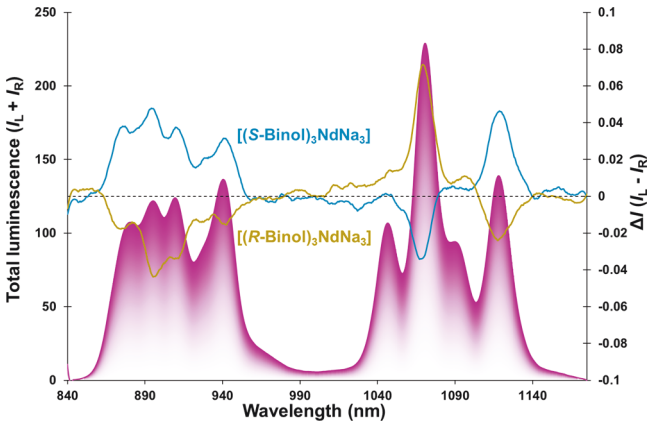

Figure 6. Normalized CPL spectra of $[(R\text{-Binol})_3NdNa_3]$ (yellow) and $[(S\text{-Binol})_3NdNa_3]$ (blue) in tetrahydrofuran solutions (1.3×10^{-3} mol L^{-1}) at room temperature. See Figure S16 for g_{lum} plot. Total luminescence is traced in the background. Excitation at 380 nm. Bandpass: 10 nm.

We have synthesized molecular lanthanide complexes $[(Binol)_3LnNa_3]$ (Ln = Er, Yb, and Nd) emitting CPL in the NIR (see Table 1 for a summary of the data). The erbium complexes synthesized here are the first reported examples of CPL observed beyond 1200 nm, and the emission is importantly centered within the 1550 nm telecom band. Additionally, the CPL magnitudes observed are exceptionally high ($|g_{lum}| = 0.47$). Strong CPL is also observed for the ytterbium analogues, with an improvement of two orders of magnitude for their CPL brightness. We also observed that the cation significantly impacts CPL magnitude. Thorough cation/CPL activity relationship studies complemented by theoretical calculations are currently ongoing in our laboratories. Owing to the simplicity and tunability of the present system, we predict a bright future for CPL active NIR emitters beyond 1200 nm.

Table 1. Summary of the Photophysical Properties of $[(Binol)_3LnNa_3]$

Ln	λ (nm)	ε (M^{-1} cm^{-1})	Φ	transition	$\lvert g_{lum}\rvert$	B_{CPL} (M^{-1} cm^{-1})
Er	1540	42 000	0.0058	$^4I_{13/2} \rightarrow {}^4I_{15/2}$	0.47	57.3
Yb	975	26 000	0.17	$^2F_{5/2} \rightarrow {}^2F_{7/2}$	0.17	379
Nd	900	35 000	0.093	$^4F_{3/2} \rightarrow {}^4I_{9/2}$	0.04	28.6
	1040			$^4F_{3/2} \rightarrow {}^4I_{11/2}$	0.03	23.9

■ ASSOCIATED CONTENT

Supporting Information

The Supporting Information is available free of charge at https://pubs.acs.org/doi/10.1021/jacs.2c01134.

General information, synthetic details, additional chiroptical characterization, crystallographic parameters (PDF)

https://doi.org/10.1021/jacs.2c01134
J. Am. Chem. Soc. 2022, 144, 6148−6153

Accession Codes

CCDC 2144209−2144210 contain the supplementary crystallographic data for this paper. These data can be obtained free of charge via www.ccdc.cam.ac.uk/data_request/cif, or by emailing data_request@ccdc.cam.ac.uk, or by contacting The Cambridge Crystallographic Data Centre, 12 Union Road, Cambridge CB2 1EZ, UK; fax: +44 1223 336033.

AUTHOR INFORMATION

Corresponding Author

Gaël Ung − *Department of Chemistry, University of Connecticut, Storrs, Connecticut 06269, United States;* orcid.org/0000-0002-6313-3658; Email: gael.ung@uconn.edu

Authors

Nishya F. M. Mukthar − *Department of Chemistry, University of Connecticut, Storrs, Connecticut 06269, United States;* orcid.org/0000-0001-7222-6576

Nathan D. Schley − *Department of Chemistry, Vanderbilt University, Nashville, Tennessee 37235, United States;* orcid.org/0000-0002-1539-6031

Complete contact information is available at: https://pubs.acs.org/10.1021/jacs.2c01134

Notes

The authors declare no competing financial interest.

ACKNOWLEDGMENTS

This material is based upon work supported by the National Science Foundation under Grant No. CHE-2041084. We thank the College of Liberal Arts and Sciences at the University of Connecticut for partial support through its Equipment Initiative Grant. We thank Samantha Rubio for assistance with PXRD measurements.

REFERENCES

(1) Addanki, S.; Amiri, I. S.; Yupapin, P. Review of optical fibers-introduction and applications in fiber lasers. *Result in phys.* **2018**, *10* (8), 743−750.

(2) Simon, C. Towards a global quantum network. *Nat. Photonics* **2017**, *11* (11), 678−680.

(3) Li, X.; Voss, P. L.; Sharping, J. E.; Kumar, P. Optical-Fiber Source of Polarization-Entangled Photons in the 1550 nm Telecom Band. *Phys. Rev. Lett.* **2005**, *94* (5), 053601-1−053601-4.

(4) Sánchez-Carnerero, E. M.; Agarrabeitia, A. R.; Moreno, F.; Maroto, B. L.; Muller, G.; Ortiz, M. J.; de la Moya, S. Circularly Polarized Luminescence from Simple Organic Molecules. *Chem. Eur. J.* **2015**, *21* (39), 13488−13500. (b) Di Bari, L.; Zinna, F. Lanthanide Circularly Polarized Luminescence: Bases and Applications. *Chirality* **2015**, *27* (1), 1−13. (c) Carr, R.; Evans, N. H.; Parker, D. Lanthanide complexes as chiral probes exploiting circularly polarized luminescence. *Chem. Soc. Rev.* **2012**, *41* (23), 7673−7686. (d) Muller, G. Luminescent chiral lanthanide(iii) complexes as potential molecular probes. *Dalton Trans.* **2009**, No. 44, 9692−9707. (e) Dhbaibi, K.; Favereau, L.; Crassous, J. Enantioenriched Helicenes and Helicenoids Containing Main-Group Elements (B, Si, N, P). *Chem. Rev.* **2019**, *119* (14), 8846−8953. (f) Zhang, D.-W.; Li, M.; Chen, C.-F. Recent advances in circularly polarized electroluminescence based on organic light-emitting diodes. *Chem. Soc. Rev.* **2020**, *49*, 1331−1343.

(5) (a) Farshchi, R.; Ramsteiner, M.; Herfort, J.; Tahraoui, A.; Grahn, H. T. Optical Communication of Spin Information Between Light Emitting Diodes. *Appl. Phys. Lett.* **2011**, *98* (16), 162508-1−162508-3. (b) Sherson, J. F.; Krauter, H.; Olsson, R. K.; Julsgaard, B.; Hammerer, K.; Cirac, I.; Polzik, E. S. Quantum Teleportation Between Light and Matter. *Nature* **2006**, *443* (7111), 557−560.

(6) Mackenzie, L. E.; Pal, R. Circularly polarized lanthanide luminescence for advanced security inks. *Nature reviews chemistry* **2021**, *5* (2), 109−124.

(7) Schadt, M. Liquid Crystal Materials and Liquid Crystal Displays. *Annu. Rev. Mater. Sci.* **1997**, *27* (1), 305−379.

(8) Lunkley, J. L.; Shirotani, D.; Yamanari, K.; Kaizaki, S.; Muller, G. Extraordinary Circularly Polarized Luminescence Activity Exhibited by Cesium Tetrakis(3-heptafluoro-butylryl-(+)-camphorato) Eu(III) Complexes in EtOH and CHCl3 Solutions. *J. Am. Chem. Soc.* **2008**, *130* (42), 13814−13815.

(9) Richardson, F. S. Selection Rules for Lanthanide Optical Activity. *Inorg. Chem.* **1980**, *19* (9), 2806−2812.

(10) Deng, M.; Schley, N. D.; Ung, G. High circularly polarized luminescence brightness from analogues of Shibasaki's lanthanide complexes. *Chem. Commun.* **2020**, *56* (94), 14813−14816.

(11) (a) Shibasaki, M.; Yoshikawa, N. Lanthanide Complexes in Multifunctional Asymmetric Catalysis. *Chem. Rev.* **2002**, *102* (6), 2187−2209. (b) Shibasaki, M.; Kanai, M.; Matsunaga, S.; Kumagai, N. Recent Progress in Asymmetric Bifunctional Catalysis Using Multimetallic Systems. *Acc. Chem. Res.* **2009**, *42* (8), 1117−1127. (c) Wooten, A. J.; Salvi, L.; Carroll, P. J.; Walsh, P. J. Characterization of Dimeric and Tetrameric μ-Hydroxide Ytterbium(III) Binaphtholate Complexes. *Adv. Synth. Catal.* **2007**, *349* (4−5), 561−565. (d) Wooten, A. J.; Carroll, P. J.; Walsh, P. J. Evidence for Substrate Binding by the Lanthanide Centers in $[Li_3(thf)_n(binolate)_3Ln]$: Solution and Solid-State Characterization of Seven- and Eight-Coordinate $[Li_3(sol)_n(binolate)_3Ln(S)_m]$ Adducts. *Angew. Chem., Int. Ed.* **2006**, *45* (16), 2549−2552. (e) Wooten, A. J.; Carroll, P. J.; Walsh, P. J. Impact of Na− and K−C π-Interactions on the Structure and Binding of $M_3(sol)_n(BINOLate)_3Ln$ Catalysts. *Org. Lett.* **2007**, *9* (17), 3359−3362. (f) Wooten, A. J.; Carroll, P. J.; Walsh, P. J. Insight into Substrate Binding in Shibasaki's $Li_3(THF)_n(BINOLate)_3Ln$ Complexes and Implications in Catalysis. *J. Am. Chem. Soc.* **2008**, *130*, 7407−7419. (g) Di Bari, L.; Lelli, M.; Pintacuda, G.; Pescitelli, G.; Marchetti; Salvadori, F. Solution versus Solid-State Structure of Ytterbium Heterobimetallic Catalysts. *J. Am. Chem. Soc.* **2003**, *125* (18), 5549−5558. (h) Di Bari, L.; Lelli, M.; Salvadori, P. Ligand Lability and Chirality Inversion in Yb Heterobimetallic Catalysts. *Chem. -Eur. J.* **2004**, *10* (18), 4594−4598. (i) Panetti, G. B.; Varela, E. J.; Gau, M. R.; Schelter, E. J.; Walsh, P. J. An investigation of the binding of (*S*)-monothioBINOLate to rare earth metal cations. *Phosphorus, Sulfur, Silicon Relat. Elem.* **2019**, *194* (7), 624−629. (j) Panetti, G. B.; Robinson, J.; Carroll, P. J.; Gau, M. R.; Manor, B. C.; Walsh, P. J.; Schelter, E. J. Synthesis of novel copper-rare earth BINOLate frameworks from a hydrogen bonding DBU-H rare earth BINOLate complex. *Dalton Trans.* **2018**, *47* (41), 14408−14410. (k) Robinson, J. R.; Qiao, Y.; Gu, J.; Carroll, P. J.; Walsh, P. J.; Schelter, E. J. The role of dynamic ligand exchange in the oxidation chemistry of cerium(III). *Chem. Sci.* **2016**, *7* (7), 4537−4547. (l) Robinson, J. R.; Gu, J.; Carroll, P. J.; Schelter, E. J.; Walsh, P. J. Exchange Processes in Shibasaki's Rare Earth Alkali Metal BINOLate Frameworks and Their Relevance in Multifunctional Asymmetric Catalysis. *J. Am. Chem. Soc.* **2015**, *137* (22), 7135−7144. (m) Yadav, J.; Stanton, G. R.; Fan, X.; Robinson, J. R.; Schelter, E. J.; Walsh, P. J.; Pericas, M. A. Asymmetric Allylation of Ketones and Subsequent Tandem Reactions Catalyzed by a Novel Polymer-Supported Titanium−BINOLate Complex. *Chem. Eur. J.* **2014**, *20* (23), 7122−7127. (n) Robinson, J. R.; Fan, X.; Yadav, J.; Carroll, P. J.; Wooten, A. J.; Pericàs, M. A.; Schelter, E. J.; Walsh, E. J. Air- and Water-Tolerant Rare Earth Guanidinium BINOLate Complexes as Practical Precatalysts in Multifunctional Asymmetric Catalysis. *J. Am. Chem. Soc.* **2014**, *136* (22), 8034−8041. (o) Nieto, I.; Wooten, A.; Robinson, J. R.; Carroll, P. J.; Schelter, E. J.; Walsh, P. J. Synthesis and Catalytic Activity of Heterobimetallic Rare Earth−Zinc Ethyl BINOLate Analogues of Shibasaki's Catalysts. *Organometallics* **2013**, *32* (24), 7431−7439. (p) Robinson, J. R.; Gordon, Z.; Booth, G. H.; Carroll, P. J.; Walsh, P. J.; Schelter, E. J. Tuning Reactivity and

Electronic Properties through Ligand Reorganization within a Cerium Heterobimetallic Framework. *J. Am. Chem. Soc.* **2013**, *135* (50), 19016−19024. (q) Robinson, J. R.; Booth, G. H.; Carroll, P. J.; Walsh, P. J.; Schelter, E. J. Dimeric Rare Earth BINOLate Complexes: Activation of 1,4−Benzoquinone through Lewis-Acid Promoted Potential Shifts. *Chem. -Eur. J.* **2013**, *19* (19), 5996−6004. (r) Robinson, J. R.; Carroll, P. J.; Walsh, P. J.; Schelter, E. J. Uranium(IV) BINOLate Heterobimetallics: Synthesis and Reactivity in an Asymmetric Diels−Alder Reaction. *Organometallics* **2013**, *32* (5), 1493−1499. (s) Robinson, J. R.; Carroll, P. J.; Walsh, P. J.; Schelter, E. J. The Impact of Ligand Reorganization on Cerium(III) Oxidation Chemistry. *Angew. Chem., Int. Ed.* **2012**, *124* (40), 10306−10310. (t) Panetti, G. B.; Robinson, J. R.; Schelter, E. J.; Walsh, P. J. Expanding the Rare-Earth Metal BINOLate Catalytic Multitool beyond Enantioselective Organic Synthesis. *Acc. Chem. Res.* **2021**, *54* (11), 2637−2648.

(12) (a) Amoroso, A.; Pope, S. Using lanthanide ions in molecular bioimaging. *Chem. Soc. Rev.* **2015**, *44*, 4723−4742. (b) Heffern, M.; Matosziuk, L.; Meade, T. Lanthanide Probes for Bioresponsive Imaging. *Chem. Rev.* **2014**, *114* (8), 4496−4539. (c) Hemmer, E.; Venkatachalam, N.; Hyodo, H.; Hattori, A.; Ebina, Y.; Kishimoto, H.; Soga, K. Upconverting and NIR emitting rare earth based nanostructures for NIR-bioimaging. *Nanoscale* **2013**, *5* (23), 11339−11361. (d) Bünzli, J. G. Lanthanide Luminescence for Biomedical Analyses and Imaging. *Chem. Rev.* **2010**, *110* (5), 2729−2755. (e) Parker, D.; Fradgley, J. D.; Wong, K.-L. The design of responsive luminescent lanthanide probes and sensors. *Chem. Soc. Rev.* **2021**, *50*, 8193−8213. (f) Stachelek, P.; MacKenzie, L.; Parker, D.; Pal, R. Circularly polarised luminescence laser scanning confocal microscopy to study live cell chiral molecular interactions. *Nat. Commun.* **2022**, *13*, 553.

(13) (a) Deng, M.; Schley, N. D.; Ung, G. Solvent Dependent Sensitization of Ytterbium and Neodymium via an Intramolecular Excimer. *Inorg. Chem.* **2018**, *57* (24), 15399−15405. (b) Ayers, K. M.; Schley, N. D.; Ung, G. Monometallic Lanthanide Salicylhydrazone Complexes Exhibiting Strong Near-Infrared Luminescence. *Chem. Commun.* **2019**, *55* (58), 8446−8449.

(14) Sasai, H.; Suzuki, T.; Itoh, N.; Tanaka, K.; Date, T.; Okamura, K.; Shibasaki, M. Catalytic Asymmetric Nitroaldol Reaction Using Optically Active Rare Earth BINOL Complexes: Investigation of the Catalyst Structure. *J. Am. Chem. Soc.* **1993**, *115* (22), 10372−10373.

(15) (a) Sun, Q.; Yan, P.; Niu, W.; Chu, W.; Yao, X.; An, G.; Li, G. NIR luminescence of a series of benzoyltrifluoroacetone erbium complexes. *RSC Adv.* **2015**, *5* (81), 65856−65861. (b) Song, L.; Hu, J.; Wang, J.; Liu, X.; Zhen, Z. Novel perfluorodiphenylphosphinic acid lanthanide (Er or Er−Yb) complex with high NIR photoluminescence quantum yield. *Photochem. Photobiol. Sci.* **2008**, *7* (6), 689−693. (c) Li, Y.; Yang, H.; He, Z.; Liu, L.; Wang, W.; Li, F.; Xu, L. Significant Increment of Photoluminescence Quantum Yield by Efficiently Prohibiting Fluorescence Quenching in Erbium(III) Organic Complexes. *J. Mater. Res.* **2005**, *20* (11), 2940−2946. (d) Nah, M.-K.; Cho, H.-G.; Kwon, H.-J.; Kim, Y.-J.; Park, C.; Kim, H. K.; Kang, J.-G. Photophysical Properties of Near-Infrared-Emitting Ln(III) Complexes with 1-(9-Anthryl)-4,4,4-trifluoro-1,3-butandione (Ln) Nd and Er). *J. Phys. Chem. A* **2006**, *110* (35), 10371−10374. (e) Zhang, J.; Petoud, S. Azulene-Moiety-Based Ligand for the Efficient Sensitization of Four Near-Infrared Luminescent Lanthanide Cations: Nd3+, Er3+, Tm3+, and Yb3+. *Chem. -Eur. J.* **2008**, *14* (4), 1264−1272. (f) Ahmed, Z.; Iftikhar, K. Sensitization of Visible and NIR Emitting Lanthanide(III) Ions in Noncentrosymmetric Complexes of Hexafluoroacetylacetone and Unsubstituted Monodentate Pyrazole. *J. Phys. Chem. A* **2013**, *117* (44), 11183−11201. (g) Lama, M.; Mamula, O.; Kottas, G.; Rizzo, F.; De Cola, L.; Nakamura, A.; Kuroda, R.; Stoeckli-Evans, H. Lanthanide Class of a Trinuclear Enantiopure Helical Architecture Containing Chiral Ligands: Synthesis, Structure, and Properties. *Chem. -Eur. J.* **2007**, *13* (26), 7358−7373. (h) Hua, K. T.; Xu, J.; Quiroz, E. E.; Lopez, S.; Ingram, A. J.; Johnson, V. A.; Tisch, A. R.; de Bettencourt-Dias, A.; Straus, D. A.; Muller, G. Structural and Photophysical Properties of Visible- and Near-IR-Emitting Tris Lanthanide(III) Complexes Formed with the Enantiomers of N,N′-Bis(1-phenylethyl)-2,6-pyridinedicarboxamide. *Inorg. Chem.* **2012**, *51* (1), 647−660. (i) Shen, H.; Berezin, A. S.; Antonova, O. V.; Zvereva, V. V.; Korolkov, I. V.; Pervukhina, N. V.; Prokhorova, S. A.; Stabnikov, P. A. Crystal Structures of $[Dy(dpm)_3]_2$ and $Dy(dpm)_3$, Luminescent and X-Ray Fluorescent Study of Lanthanide(III) *Tris*-Dipivaloylmethanates. *J. Struct. Chem.* **2018**, *59* (3), 676−683.

(16) (a) Ning, Y.; Tang, J.; Liu, Y.; Jing, J.; Sun, Y.; Zhang, J. Highly luminescent, biocompatible ytterbium(III) complexes as near-infrared fluorophores for living cell imaging. *Chem. Sci.* **2018**, *9* (15), 3742−3753. (b) Han, Q.; Wang, L.; Shi, Z.; Xu, C.; Dong, Z.; Mou, Z.; Liu, W. Self-Assembly of Luminescent Lanthanide Mesocates as Efficient Catalysts for Transforming Carbon Dioxide into Cyclic Carbonates. *Chem. Asian J.* **2017**, *12* (12), 1364−1373. (c) Utochnikova, V.; Kovalenko, A.; Burlov, A.; Marciniak, L.; Ananyev, I.; Kalyakina, A.; Kurchavov, N.; Kuzmina, N. Lanthanide complexes with 2-(tosylamino)benzylidene-N-benzoylhydrazone, which exhibit high NIR emission. *Dalton Trans.* **2015**, *44* (28), 12660−12669. (d) Tang, M.; Huang, Y.; Wang, Y.; Fu, L. An ytterbium complex with unique luminescence properties: detecting the temperature based on a luminescence spectrum without the interference of oxygen. *Dalton Trans.* **2015**, *44* (16), 7449−7457. (e) Li, B.; Li, H.; Chen, P.; Sun, W.; Wang, C.; Gao, T.; Yan, P. Enhancement of near-infrared luminescence of ytterbium in triple-stranded binuclear helicates. *Phys. Chem. Chem. Phys.* **2015**, *17* (45), 30510−30517. (f) Ke, X.; Yang, B.; Cheng, X.; Chan, S.; Zhang, J. Ytterbium(III) Porpholactones: b-Lactonization of Porphyrin Ligands Enhances Sensitization Efficiency of Lanthanide Near-Infrared Luminescence. *Chem. -Eur. J.* **2014**, *20*, 4324−4333. (g) Comby, S.; Tuck, S.; Truman, L.; Kotova, O.; Gunnlaugsson, T. New Trick for an Old Ligand! The Sensing of Zn(II) Using a Lanthanide Based Ternary Yb(III)-cyclen-8-hydroxyquinoline System As a Dual Emissive Probe for Displacement Assay. *Inorg. Chem.* **2012**, *51* (19), 10158−10168. (h) Ilichev, V. A.; Silantyeva, L. I.; Yablonskiy, A. N.; Andreev, B. A.; Rumyantcev, R. V.; Fukin, G. K.; Bochkarev, M. N. Synthesis, structure and long-lived NIR luminescence of lanthanide ate complexes with perfluorinated 2-mercaptobenzothiazole. *Dalton Trans.* **2019**, *48* (3), 1060−1066. (i) Pushkarev, A. P.; Balashova, T. V.; Kukinov, A. A.; Arsenyev, M. V.; Yablonskiy, A. N.; Kryzhkov, D. I.; Andreev, B. A.; Rumyantcev, R. V.; Fukin, G. K.; Bochkarev, M. N. Sensitization of NIR luminescence of Yb^{3+} by Zn^{2+} chromophores in heterometallic complexes with a bridging Schiff-base ligand. *Dalton Trans.* **2017**, *46* (31), 10408−10417. (j) Hu, J.; Ning, Y.; Meng, Y.; Zhang, J.; Wu, Z.; Gao, S.; Zhang, J. Highly near-IR emissive ytterbium(III) complexes with unprecedented quantum yields. *Chem. Sci.* **2017**, *8* (4), 2702−2709.

(17) (a) Congiu, M.; Alamiry, M.; Moudam, O.; Ciorba, S.; Richardson, P. R.; Maron, L.; Jones, A. C.; Richards, B. S.; Robertson, N. Preparation and photophysical studies of [Ln(hfac)3DPEPO], Ln = Eu, Tb, Yb, Nd, Gd; interpretation of total photoluminescence quantum yields. *Dalton Trans.* **2013**, *42* (37), 13537−13545. (b) Ryo, M.; Wada, Y.; Okubo, T.; Yanagida, S. Near-IR emission of Nd(III) encaged in nanosized zeolites. *Res. Chem. Intermediat.* **2004**, *30* (2), 191−205. (c) Hasegawa, Y.; Murakoshi, K.; Wada, Y.; Kim, J.; Nakashima, N.; Yamanaka, T.; Yanagida, S. Characteristic emission of *β*-diketonato Nd3+ complexes dressed with perfluoroalkyl groups in DMSO-d6. *Chemical physical letters* **1996**, *260* (1), 173−177.

(18) Willis, O. G.; Zinna, F.; Pescitelli, G.; Micheletti, C.; Di Bari, L. Remarkable near-infrared chiroptical properties of chiral Yb, Tm and Er complexes. *Dalton Trans.* **2022**, *51* (2), 518−523.

(19) (a) Zinna, F.; Arrico, L.; Di Bari, L. Near-infrared circularly polarized luminescence from chiral Yb(iii)-diketonates. *Chem. Commun.* **2019**, *55* (46), 6607−6609. (b) Dickins, R. S.; Howard, J. A. K.; Maupin, C. L.; Moloney, J. M.; Parker, D.; Riehl, J. P.; Siligardi, G.; Williams, J. A. G. Synthesis, Time-Resolved Luminescence, NMR Spectroscopy, Circular Dichroism and Circularly Polarised Luminescence Studies of Enantiopure Macrocyclic Lanthanide Tetraamide Complexes. *Chem. -Eur. J.* **1999**, *5* (3), 1095−1105. (c) Walton, J. W.; Carr, R.; Evans, N. H.; Funk, A. M.;

https://doi.org/10.1021/jacs.2c01134
J. Am. Chem. Soc. 2022, 144, 6148−6153

Kenwright, A. M.; Parker, D.; Yufit, D. S.; Botta, M.; De Pinto, S.; Wong, K. Isostructural Series of Nine-Coordinate Chiral Lanthanide Complexes Based on Triazacyclononane. *Inorg. Chem.* **2012**, *51* (15), 8042−8056. (d) Lefeuvre, B.; Mattei, C. A.; Gonzalez, J. F.; Gendron, F.; Dorcet, V.; Riobé, F.; Lalli, C.; Le Guennic, B.; Cador, O.; Maury, O.; Guy, S.; Bensalah-Ledoux, A.; Baguenard, B.; Pointillart, F. Solid-State Near-Infrared Circularly Polarized Luminescence from Chiral Yb^{III}-Single-Molecule Magnet. *Chem. -Eur. J.* **2021**, *27* (26), 7362−7366. (e) Maupin, C. L.; Dickins, R. S.; Govenlock, L. G.; Mathieu, C. E.; Parker, D.; Williams, J. A. G.; Riehl, J. P. The Measurement of Circular Polarization in the Near-IR Luminescence from Chiral Complexes of Yb(III) and Nd(III). *J. Phys. Chem. A* **2000**, *104* (29), 6709−6717. (f) Berardozzi, R.; Di Bari, L. Optical Activity in the Near-IR Region: The λ=980 nm Multiplet of Chiral Yb^{3+} Complexes. *ChemPhysChem* **2015**, *16* (13), 2868−2875. (g) Gendron, F.; Di Pietro, S.; Abad Galán, L.; Riobé, F.; Placide, V.; Guy, L.; Zinna, F.; Di Bari, L.; Bensalah-Ledoux, A.; Guyot, Y.; Pilet, G.; Pointillart, F.; Baguenard, B.; Guy, S.; Cador, O.; Maury, O.; Le Guennic, B. Luminescence, chiroptical, magnetic and ab initio crystal-field characterizations of an enantiopure helicoidal Yb(iii) complex. *Inorg. Chem. Front.* **2021**, *8* (4), 914−926. (h) Wu, T.; Kapitán, J.; Andrushchenko, V.; Bouř, P. Identification of Lanthanide(III) Luminophores in Magnetic Circularly Polarized Luminescence Using Raman Optical Activity Instrumentation. *Anal. Chem.* **2017**, *89* (9), 5043−5049. (i) Wu, T.; Bour, P. Specific circularly polarized luminescence of Eu(iii), Sm(iii), and Er(iii) induced by N-acetylneuraminic acid. *Chem. Commun.* **2018**, *54* (14), 1790−1792. (j) Bing, T. Y.; Kawai, T.; Yuasa, J. Ligand-to-Ligand Interactions That Direct Formation of D2-Symmetrical Alternating Circular Helicate. *J. Am. Chem. Soc.* **2018**, *140* (10), 3683−3689. (k) Dai, L.; Jones, C. M.; Chan, W. T. K.; Pham, T. A.; Ling, X.; Gale, E. M.; Rotile, N. J.; Tai, W. C.; Anderson, C. J.; Caravan, P.; Law, G. Chiral DOTA chelators as an improved platform for biomedical imaging and therapy applications. *Nat. Commun.* **2018**, *9* (1), 857. (l) Dai, J.; Zhang, J.; Chen, Y.; Mackenzie, M. E.; Pal, R.; Law, G.-L. Synthesis of Water-Soluble Chiral DOTA Lanthanide Complexes with Predominantly Twisted Square Antiprism Isomers and Circularly Polarized Luminescence. *Inorg. Chem.* **2019**, *58* (19), 12506−12510. (m) Maupin, C. L.; Parker, D.; Williams, J. A. G.; Riehl, J. P. Circularly Polarized Luminescence from Chiral Octadentate Complexes of Yb(III) in the Near-Infrared. *J. Am. Chem. Soc.* **1998**, *120* (40), 10563−10564.

(20) Perkins, W. G.; Crosby, G. A. Crystal-Field Splitting in Yb^{3+} Chelates. *J. Chem. Phys.* **1965**, *42* (1), 407−414.

(21) Di Bari, L.; Lelli, M.; Pintacuda, G.; Pescitelli, G.; Marchetti, F.; Salvadori, P. Solution versus Solid-State Structure of Ytterbium Heterobimetallic Catalysts. *J. Am. Chem. Soc.* **2003**, *125* (18), 5549−5558.

(22) Arrico, L.; Di Bari, L.; Zinna, F. Quantifying the overall efficiency of circularly polarized emitters. *Chem. -Eur. J.* **2021**, *27* (9), 2920−2934.

Recommended by ACS

Steric and Electronic Control of Chiral Eu(III) Complexes for Effective Circularly Polarized Luminescence

Yuichi Kitagawa, Yasuchika Hasegawa, *et al.*

FEBRUARY 07, 2020
ACS OMEGA

READ

Circularly Polarized Luminescence from Enantiopure C_2-Symmetrical Tetrakis(2-pyridylmethyl)-1,2-diaminocyclohexane Lanthanide Complexes

Kaitlynn M. Ayers, Gaël Ung, *et al.*

MAY 19, 2020
INORGANIC CHEMISTRY

READ

Visible Circularly Polarized Luminescence of Octanuclear Circular Eu(III) Helicate

Yan Bing Tan, Tsuyoshi Kawai, *et al.*

SEPTEMBER 22, 2020
JOURNAL OF THE AMERICAN CHEMICAL SOCIETY

READ

Alkynyl-Stabilized Superatomic Silver Clusters Showing Circularly Polarized Luminescence

Miao-Miao Zhang, Thomas C. W. Mak, *et al.*

APRIL 19, 2021
JOURNAL OF THE AMERICAN CHEMICAL SOCIETY

READ

Get More Suggestions >

https://doi.org/10.1021/jacs.2c01134
J. Am. Chem. Soc. 2022, 144, 6148−6153